JOURNAL OF
AGRICULTURAL AND FOOD CHEMISTRY

Two Peptides from Soy β-Conglycinin Induce a Hypocholesterolemic Effect in HepG2 Cells by a Statin-Like Mechanism: Comparative in Vitro and in Silico Modeling Studies

Carmen Lammi,[†] Chiara Zanoni,[‡] Anna Arnoldi,*,[†] and Giulio Vistoli[†]

[†]Department of Pharmaceutical Sciences, University of Milan, via Mangiagalli 25, Milan 20133, Italy
[‡]Cardio-toraco-vascular Department, Niguarda Hospital, Milan 20162, Italy

Ⓢ Supporting Information

ABSTRACT: Two peptides from soybean β-conglycinin, i.e., YVVNPDNDEN (peptide **2**) and YVVNPDNNEN (peptide **3**), are known to be absorbed by human enterocytes. The former is a fragment of LRVPAGTTF**YVVNPDNDEN**LRMIA (peptide **1**), previously shown to increase the low-density lipoprotein (LDL) uptake and degradation in hepatocytes. Research carried out in silico on their interactions with the catalytic site of 3-hydroxy-3-methylglutaryl CoA reductase (HMGCoAR) demonstrated that they behave as competitive inhibitors of HMGCoAR activity with a statin-like mechanism, confirmed by direct inhibition experiments. Research in HepG2 cells aimed at investigating the effects of these peptides on cholesterol metabolism showed that compared to mock treatment peptide **2** at 350 μM up-regulates the mature SREBP2 protein level by $134.0 \pm 10.5\%$, increases the LDLR protein level by $152.0 \pm 20.0\%$, and enhances the HMGCoAR protein production by $171 \pm 29.9\%$, whereas peptide **3** up-regulates the mature SREBP2 protein level by $158.0 \pm 9.2\%$, increases the LDL level $164.0 \pm 17.9\%$, and induces a HMGCoAR protein increase by $170 \pm 50.0\%$.

KEYWORDS: cholesterol regulation, plant protein, HepG2 cell line, HMGCoA reductase, β-conglycinin

INTRODUCTION

The hypocholesterolemic activity of soy foods has been known for many years.[1−3] Studies in animals[4] and in humans[5,6] have demonstrated that the mechanism of action is linked to the up-regulation of low-density lipoprotein receptors (LDLR), which are relevant in the metabolic degradation of low-density lipoproteins (LDL). Other studies[7] have shown that the protein is a main bioactive soybean component. The two major components of soybean protein are glycinin, a nonglycosylated 11S globulin (legumin), and β-conglycinin, a glycosylated 7S globulin (vicilin).[8] The latter consists of different combinations of three major subunits, namely, α, α′, and β. Experimental evidence in animals[9−11] indicates that the α′ subunit has a major role in the cholesterol-lowering properties of soybean.

Because proteins are digested in the gastroenteric system, their activities should depend on the release of bioactive peptides encrypted in their sequences.[12−18] Lovati and co-workers[7] have suggested that specific peptides from β-conglycinin are important for the observed hypocholesterolemic activity. In particular, they tested LRVPAGTTFYVV-NPDNDENLRMIA (peptide **1**), corresponding to positions 301−324 of the α′ subunit of β-conglycinin (UNIProtKB: P11827), at a concentration of 10^{-4} mol/L cells and demonstrated that it increases ^{125}I-LDL uptake in human HepG2 cells by 41% and its degradation by 10% versus the vehicle. Independently, we have recently demonstrated[19] that IAVPGEVA, IAVPTGVA, and LPYP (three peptides from soy glycinin) modulate the cholesterol metabolism in HepG2 cells through activation of the low-density lipoprotein receptor (LDLR) sterol regulatory-element-binding protein 2 (SREBP2) and inhibition of 3-hydroxy-3-methylglutaryl CoA reductase

(HMGCoAR).[20] HMGCoAR is a key enzyme in the synthesis of endogenous cholesterol and the main target of statins, which interact with this enzyme as competitive inhibitors.[21]

Although in principle bioactive peptides might exert their action locally in the gastrointestinal tract, intestinal absorption prior to distribution to peripheral organs is certainly a main key factor affecting bioavailability, kinetics, and systemic actions of food peptides in vivo.[16] Interestingly, a very recent study,[22] based on a phytochemomic approach, has investigated the in vitro digestion of β-conglycinin and the potential uptake of the generated peptides by human intestinal CaCo-2 cell layers. YVVNPDNDEN (peptide **2**) and YVVNPDNNEN (peptide **3**) were among the 22 peptides transferred from the apical to the basolateral compartment in these experiments.[22] The former corresponds to positions 310−319 of the α′ subunit of β-conglycinin (UNIProtKB: P11827) and is a fragment of the above cited peptide **1** (LRVPAGTTF**YVVNPDNDEN**-LRMIA);[7] the latter is structurally very similar to peptide **1** and corresponds instead to positions 232−241 of the α subunit of β-conglycinin (UNIProtKB: P13916).

The fact that peptides **2** and **3** are bioavailable in Caco-2 cells has prompted us to investigate their interactions with the catalytic site of HMGCoAR by using molecular modeling tools and to characterize the molecular mechanism through which they potentially mediate a hypocholesterolemic effect in HepG2 cells by using a combination of molecular techniques. Finally,

again by molecular modeling, we investigated for comparison the interaction of peptide **1** with the catalytic site of HMGCoAR.

■ MATERIALS AND METHODS

Chemicals. Dulbecco's modified Eagle's medium (DMEM), L-glutamine, fetal bovine serum (FBS), phosphate-buffered saline (PBS), penicillin/streptomycin, chemiluminescent reagent, and 96-well plates were purchased from Euroclone (Milan, Italy). Bovine serum albumin (BSA), RIPA buffer, HMGCoAR assay kit, lovastatin, and the antibody against β-actin were bought from Sigma-Aldrich (St. Louis, MO, USA). The antibody against HMGCoAR was bought from Abcam (Cambridge, UK). The antibodies against SREBP-2, rabbit Ig-HRP, mouse Ig-HRP, phenylmethanesulfonylfluoride (PMSF), Na-orthovanadate inhibitors, and goat anti-rabbit Ig-HRP were purchased from Santa Cruz Biotechnology, Inc. (Santa Cruz, CA, USA). The antibodies against LDLR were bought from Pierce (Rockford, IL, USA); the inhibitor cocktail Complete Midi was purchased from Roche (Basel, Swiss). Mini protean TGX precast gel 7.5% and Mini nitrocellulose Transfer Packs were purchased from BioRad (Hercules, CA, USA). YVVNPDNDEN and YVVNPDNNEN were bought from PRIMM (Milan, Italy), which certified >95% purity by HPLC.

Computational Methods. The structures of peptides **1**−**3** were built by using two different strategies. The shortest derivatives (peptides **2** and **3**) were manually modeled in a canonical α-helix by using the Peptide Builder function of the VEGA suite of programs; then, their conformational profiles were explored by a MonteCarlo procedure, which produced 20 000 conformers by randomly rotating the backbone torsions only. The final geometries were then clustered according to their similarity to discard redundant ones; here, two conformations were considered as nonredundant when they differed by more than 60° in at least one backbone torsion angle. For each cluster, the lowest energy structure was collected and memorized. By contrast, the structure of the longest peptide (**1**) was generated by homology modeling, using the Fugue online program, on the basis of the resolved structure of phaseolin as the template (Protein Database (PDB) ID: 2PHL). This model was completed by adding side chains and hydrogen atoms and then minimized by keeping the backbone atoms fixed to preserve the predicted folding.

Among the resolved human HMG-CoA reductase structures, the study involved the complex between the enzyme and a statin (i.e., (3R,5R)-7-[2-(4-fluorophenyl)-4-{[(1S)-2-hydroxy-1-phenylethyl]-carbamoyl}-5-(1-methylethyl)-1H-imidazol-1-yl]-3,5-dihydroxyheptanoic acid, PDB ID: 3CCZ) because this showed the best resolution (1.70 Å).[21] Even though the resolved structure is a homotetramer, the simulations were focused on a functionally active homodimer, which completely encompasses the catalytic binding site. After deleting water molecules, ions, and crystallization additives, the selected dimer bound to the statin was completed by adding the hydrogen atoms and then optimized by keeping the backbone atoms fixed to preserve the resolved folding. The inhibitor was finally deleted, and the obtained protein structure underwent the following docking simulations.

Although requiring different strategies, all docking simulations were carried out by using the program Protein−Ligand ANT System (PLANTS, release 1.1),[23] which generates reliable ligand poses by using ant colony optimization algorithms (ACO).

For the shortest peptides (peptides **2** and **3**), docking simulations involved the 20 lowest energy conformations as derived by the previous MonteCarlo analysis in order to minimize the biasing effects of the starting conformation on the obtained results. In detail, the search was focused on a 15.0 Å radius sphere around the bound statin, thus including the entire binding cavity. PLANTS was used with default settings and without geometric constraints: Speed 1 was used, and 5 poses were generated and scored for each conformer by using the ChemPLP function. The obtained poses were evaluated by considering both the docking scores and the conformational energies of the docked conformers. The best poses were then minimized, keeping fixed all atoms inside a 15.0 Å radius sphere around the bound peptide. Although adopting the same computational procedures

already described, the docking study for the longest peptide **1** was focused on the single conformation as derived by homology modeling.

The computed complexes for peptide **1** and **2** underwent 10 ns molecular dynamic (MD) study. It should be noted here that the MD simulations had the primary objective of assessing the stability of the generated complexes as well as of their key stabilizing contacts and were not aimed at investigating the conformational changes induced by the bound ligand on the protein structure because this would have clearly required longer simulations. First, the complexes were embedded in a cubic box of water (85 Å × 85 Å × 85 Å) containing 16 250 solvent molecules. The systems were then minimized to optimize the relative position of the solvent molecules and then were subjected to MD runs with the following characteristics: (a) Periodic boundary conditions (95 Å × 95 Å × 95 Å) were applied to stabilize the simulation space. (b) Newton's equation was integrated using the r-RESPA method (every 4 fs for long-range electrostatic forces, 2 fs for short-range non bonded forces, and 1 fs for bonded forces). (c) The long-range electrostatic potential was computed by the Particle Mesh Ewald summation method (80 × 80 × 80 grid points). (d) The temperature was maintained at 300 ± 10 K by Langevin's algorithm. (e) Lennard-Jones (L-J) interactions were calculated with a cutoff of 10 Å, and the pair list was updated every 20 iterations. (f) A frame was memorized every 10 ps, thus generating 1000 frames. (g) No constraints were imposed on the systems. The simulations were carried out in two phases: an initial period of heating from 0 to 300 K over 300 000 iterations (300 ps, i.e., 1 K/ps) and the monitored phase of 10 ns. The mentioned minimizations were carried out using the conjugate gradient algorithm until the rms gradient was smaller than 0.01 kcal mol^{-1} Å^{-1}. All calculations were carried out by Namd2.10,[24] with the force-field CHARMm v22 and Gasteiger's atomic charges.

HMGCoAR Activity Assay. HMGCoAR (catalytic domain), NADPH, assay buffer, and substrate solution were provided in the HMGCoAR assay kit (Sigma-Aldrich, St. Louis, MO, USA). The experiments were carried out at 37 °C following the manufacturer's instructions. In particular, each reaction (200 μL) was prepared by adding the reagents in the following order: 1X assay buffer; peptide **2** (at 100, 125, 150, and 250 μM), and peptide **3** (at 150, 175, 200, and 250 μM), or vehicle (C); NADPH (4 μL); substrate solution (12 μL); and finally HMGCoAR (2 μL). Subsequently, the samples were mixed, and the absorbance at 340 nm was read by a microplate reader (Synergy H1 from Biotek, Bad Friedrichshall, Germany) at 0 and 10 min. The HMGCoA-dependent oxidation of NADPH and the inhibition properties of soy peptides were measured by the absorbance reduction, which is directly proportional to enzyme activity.

Cell Line Culture. The HepG2 cell line was bought from ATCC (HB-8065, ATCC from LGC Standards, Milan, Italy). It was cultured in high-glucose DMEM with stable L-glutamine supplemented with 10% FBS, 100 U/mL penicillin, and 100 μg/mL streptomycin (complete growth medium) and incubated at 37 °C under 5% CO$_2$ atmosphere. HepG2 cells were used for no more than 20 passages after thawing because the increase of passage number may change cell characteristics and impair assay results.

Western Blot Analysis. HepG2 (1.5 × 10^5 cells/well of a 24-well plate) were treated with peptides **2** and **3** (each 350 and 500 μM) for 24 h. After each treatment, cells were scraped in 40 μL of ice-cold lysis buffer (RIPA buffer + inhibitor cocktail + 1:100 PMSF + 1:100 Na-orthovanadate) and transferred in an ice-cold microcentrifuge tube. After centrifugation at 16 060 g for 15 min at 4 °C, the supernatant was recovered and transferred to a new ice-cold tube. Total proteins were quantified by the Bradford method, and 50 μg of total proteins were loaded on a precast 7.5% sodium dodecyl sulfate−polyacrylamide (SDS-PAGE) gel at 130 V for 45 min. Subsequently, the gel was pre-equilibrated with 0.04% SDS in H$_2$O for 15 min at room temperature (RT) and transferred to a nitrocellulose membrane (Mini nitrocellulose Transfer Packs), using a Trans-blot Turbo at 1.3 A and 25 V for 7 min. Target proteins on the milk-blocked membrane were detected by primary antibodies as follows: rabbit anti-SREBP2, anti-LDLR, anti-HMGCoAR, and anti-β-actin. Secondary antibodies conjugated with HRP and a chemiluminescent reagent were used to visualize target proteins, and their signal was quantified using the
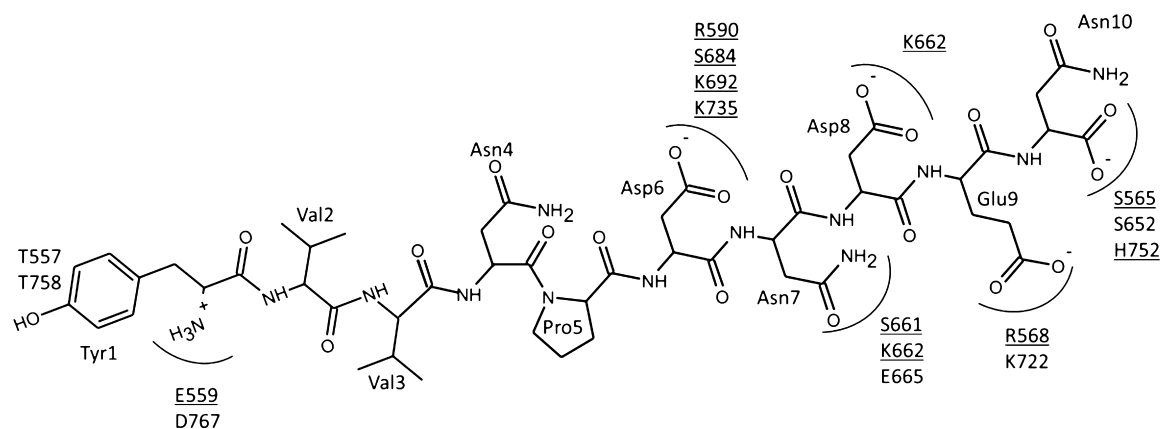
Figure 1. Bidimensional scheme reporting the key interactions stabilizing the putative complex for peptide **2**. The residues involved in the binding of the statin as found in the resolved crystal structure utilized here (PDB ID: 3CCZ) are underlined.

ImageJ Software. The internal control β-actin was used to normalize loading variations.

Fluorescent LDL Uptake Cell-Based Assay. A total of 3×10^4 HepG2 cells were seeded per well of 96-well plates and kept in complete growth medium for 2 days before treatment. On the third day, cells were treated with peptide **2** and **3** at the concentrations of 50 and 100 μM, respectively, or mock treatment (H_2O) for 24 h. At the end of the treatment period, the culture medium was replaced with 50 μL/well LDL-DyLight 550 working solution (Cayman Chemical Company, Ann Arbor, Michigan, USA). The cells were additionally incubated for 2 h at 37 °C; then, the culture medium was aspirated, washed, and replaced with PBS (100 μL/well). The degree of LDL uptake was measured using the Synergy H1 fluorescent plate reader from Biotek (excitation and emission wavelengths 540 and 570 nm, respectively).

Statistical Analysis. Statistical analyses were carried out by one-way ANOVA (Graphpad Prism 6) followed by Dunnett's test and/or t test. Values were expressed as means ± SEM; P values < 0.05 were considered to be significant.

■ RESULTS

Molecular Modeling Investigation. An in silico modeling study was undertaken to investigate the potential interaction of peptides **1**−**3** with the catalytic domain of HMGCoAR. Figure 1 shows a bidimensional scheme summarizing the key interactions stabilizing the putative complex between peptide **2** and the enzymatic cavity of HMGCoAR, whereas Figure S1A gives an overall view of the pose of peptide **2** within the HMGCoAR displayed by cartoon. Notably, most key polar interactions are elicited by the last five residues of the C terminus, whereas the first N-terminal residues are mostly involved in hydrophobic contact, with the exception of the N-terminal ammonium head, which is engaged in ionic interactions with Glu559 and Asp767, and the phenolic function of Tyr1, which stabilizes H bonds with Thr557 and Thr758. In detail, Asp6, Asp8, and Glu9 are engaged in an extended network of ion pairs involving the rich set of positively charged residues, which characterize the catalytic pocket of HMGCoAR and surround the C-terminal portion of the bound peptide, whereas the carboxyl terminus and Asn6 elicit only H bonds.

Figure 1 highlights (underlined) the residues stabilizing the key contacts with the peptide **2** that were also found to be involved in the stabilization of the experimentally resolved complex between HMGCoAR and a statin. Notably, the underlined residues mostly interact with the negatively charged C-terminal portion of peptide **2**, thus confirming that this segment is primarily involved in the inhibition of HMGCoAR by mimicking most of the polar interactions already seen for the binding of the statin polar moieties. In contrast, the hydrophobic N-terminal portion is inserted in a deeper and rather apolar subpocket that does not match that accommodating the statin hydrophobic moieties but rather roughly corresponds to that harboring the NADPH cofactor. Indeed, the statin polar groups interact with the residues contacting the HMG groups, whereas the statin apolar moieties are accommodated in the apolar subpocket interacting with the pantothenic acid moiety of CoA, and no region of the NADP(H) binding site is engaged by statins. Here, a different arrangement is observed because the hydrophobic portion of peptide **2** is partly accommodated in the elongated binding cavity of the cofactor, thus suggesting that it may also affect the NADPH binding. Similar docking simulations of peptide **3** revealed that the mutation Asp8 into Asn8 does not markedly affect the interaction pattern because Asn8 elicits H bonds with Lys662 (already seen for peptide **2**) and Glu665 (complex not shown).

Figure S1B shows the pose of peptide **1** and suggests the β-hairpin motif stabilized by several intramolecular polar contacts, among which the salt bridge between the two ionized termini has a key role in determining such a folded structure. Figure S1B also reveals that this longer peptide is accommodated within a more superficial region of the binding cavity compared to peptide **2**, and its inhibition can be due to a sort of lid mechanism involving additional regions adjacent to the rim of the catalytic pocket.

Figure S2 is a schematic representation of the key contacts stabilizing the putative complex as computed for the longer peptide **1**. Similar to what was seen for the shorter derivative, Figure S2 reveals that the conserved portion between Asp15 and Asn19 is involved in the key polar interactions with the ionizable residues lining the HMGCoAR binding cavity. Apart from Arg21, which stabilizes two ion pairs with Glu559 and Asp767, the remaining residues are generally engaged in an extended network of intramolecular and intermolecular hydrophobic contacts that contribute to the overall stabilization of the obtained complex. Remarkably, there are some residues (highlighted in green), especially in the N-terminal region, that are exclusively involved in intramolecular contacts. One may imagine that such intramolecular interactions can play a dual role because they stabilize the folded conformation and shield some unfit side chains, thus minimizing potential repulsing

contacts with surrounding enzyme residues (as in the case of Arg2).

A primary objective of the MD simulations thus carried out was to assess the stability of the computed complexes. Hence, Figure 2 compares the rmsd values of the two bound peptides
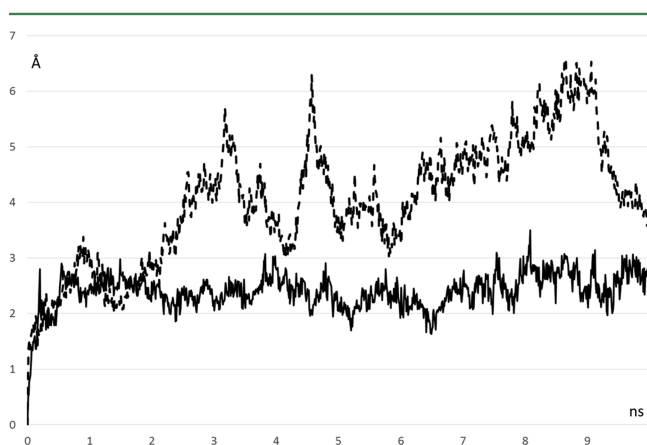
Figure 2. Rmsd profiles for the simulated peptides bound to the enzyme as derived by MD runs considering the backbone atoms only (solid black line = peptide **1**, dashed black line = peptide **2**).

as computed during the MD runs considering only the backbone atoms. It reveals two markedly different profiles because peptide **2** shows a low and rather constant profile, which is suggestive of a very stable complex in which most residues are tightly involved in key contacts. Figure S3A reports the rmsd values as dissected per residue and computed considering all atoms and confirms the key role of the ionized residues, which indeed remains nearly fixed during all the MD run.

In contrast, peptide **1** shows a higher and more variable profile, which may suggest that not all residues are equally involved in the key contacts and that some portions of peptide **1** conserve a notable mobility even within the HMGCoAR binding cavity. To better investigate this finding, Figure S3B shows the rmsd values as dissected per residue and reveals a significant variability between the thus-computed rmsd values in line with the number of polar contacts elicited by each residue. In detail, Figure S3 confirms that the region between Asn13 and Arg21 plays a key role in complex stabilization and indeed remains stably bound to the enzyme, whereas the segment between Ala5 and Val12 is engaged at most in apolar contacts and is arranged in a more superficial region of the HMGCoAR binding cavity, thus conserving a marked mobility during the MD simulation. The two terminal segments show an intermediate flexibility probably due to the ionic contact between the two terminal ionized groups. Overall, these results suggest that the computed pose of peptide **1** is stable even though a such an extended peptide cannot be completely stabilized within the enzyme catalytic site, thus explaining the observed residual flexibility.

The satisfactory stability of the two simulated complexes is further confirmed by the dynamic profile of some representative contacts as derived from MD runs and compiled in Table 1. Indeed, the reported distance values emphasize that most key ionic contacts are completely stable because the corresponding distances are comprised in very narrow ranges.

Peptides 2 and 3 Inhibit the HMGCoAR in Vitro. The experimental characterization of the molecular mechanism

Table 1. Dynamic profile of some representative contacts as derived from MD runs for the two simulated complexes[a]

| interaction	distance mean	distance minimum	distance maximum
	Peptide **2**		
$NH_3^+ \rightarrow$ E559	2.94 ± 0.095	2.69	3.45
$NH_3^+ \rightarrow$ D767	2.89 ± 0.11	2.61	3.31
Tyr1 → T557	7.84 ± 2.97	2.99	13.76
Asp6 → R590	5.04 ± 0.59	3.49	6.55
Asp6 → K692	3.08 ± 0.29	2.63	4.16
Asp6 → K735	3.04 ± 0.13	2.71	3.71
Asp8 → K662	3.16 ± 0.33	2.62	4.05
	Peptide **1**		
Asp17 → R568	3.74 ± 0.14	3.37	4.31
Glu18 → R590	4.19 ± 0.26	3.42	4.89
Asn19 → R590	4.75 ± 1.29	2.67	8.06
Arg21 → E559	3.96 ± 0.14	3.53	4.59
Arg21 → D767	6.52 ± 0.49	4.69	7.77

[a]All distances are expressed in angstroms.

through which peptides **2** and **3** may potentially mediate a hypocholesterolemic effect was carried out in two steps: first, evaluating their capacity to inhibit the catalytic activity of HMGCoAR; second, investigating in HepG2 cells how they modulate cholesterol metabolism and modify the LDL uptake. To confirm that indeed peptides **2** and **3** inhibit the catalytic activity of HMGCoAR as their main molecular target, an in vitro assay was carried out using the purified catalytic domain of this enzyme. A concentration range from 100 and 250 μM was tested. Each peptide inhibited HMGCoAR activity in a dose-dependent manner, with an IC_{50} of about 150 and 200 μM for peptides **2** and **3**, respectively (Figure 3). On the basis of these results, we decided to treat HepG2 cells in the following experiments at slightly higher concentrations, i.e., 350 and 500 μM.

Peptides 2 and 3 Induce the LDLR-SREBP2 Pathway. To verify the consequences of the HMGCoAR inhibition activity exerted by peptides **2** and **3** on the modulation of the LDLR-SREBP2 pathway, HepG2 cells were treated with both peptides at the concentrations of 350 and 500 μM, and each sample was investigated with immunoblotting experiments. Figure 4A−D shows that the treatment with each peptide induced an up-regulation of the N-terminal fragment of the SREBP2 protein level (mature form with a molecular weight of 68 kDa). In particular, peptide **2** up-regulated the mature SREBP2 protein level by 134.0 ± 10.5 and 141.1 ± 18.0% at 350 and 500 μM, respectively, whereas peptide **3** up-regulated the mature SREBP2 protein level by 158.0 ± 9.2 and by 155.2 ± 14.6% at 350 and 500 μM, respectively, versus the untreated sample.

In the same experiments, the LDLR and HMGCoAR protein level variations were also measured by immunoblotting (Figure 4B,C). All peptides increased the LDLR and HMGCoAR protein levels, in agreement with their capacity to up-regulate the transcriptional active SREBP2 fragment (mature-SREBP2) protein level. In particular, peptide **2** increased the LDLR protein level by 152.0 ± 20.0 and 167.0 ± 31.7% and peptide **3** by 164.0 ± 17.9 and 182.2 ± 41.8% versus the untreated sample at 350 and 500 μM, respectively (Figure 4E). Peptide **2** enhanced the production of the HMGCoAR protein by 171 ± 29.9 and by 187 ± 34.6% versus the untreated sample at 350 and 500 μM, respectively, whereas peptide **3** induced an
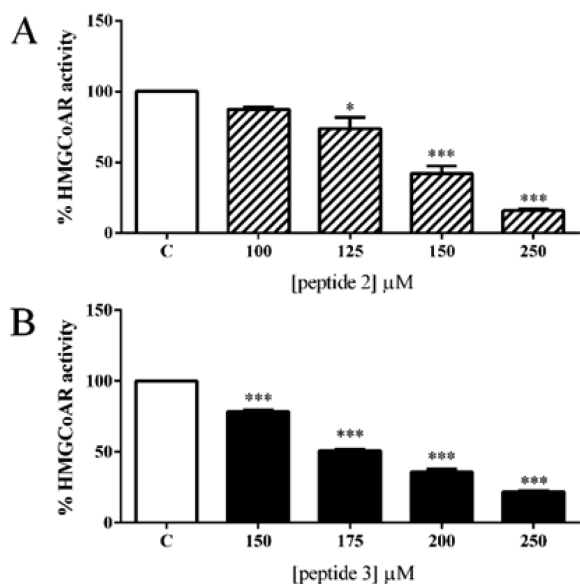
Figure 3. Effects of peptides **2** and **3** on the catalytic domain of HMGCoAR. Bars indicate the effects on the HMGCoAR activity of (A) peptide **2** (100, 125, 150, and 250 μM) and (B) peptide **3** (150, 175, 200, and 250 μM). The HMGCoAR physiologically catalyzes the four-electron reduction of HMGCoA to coenzyme A (CoA) and mevalonate (HMGCoA + 2NADPH + 2H$^+$ → mevalonate +2NADP$^+$ + CoA-SH). In this assay, the absorbance decrease at 340 nm, which represents the oxidation of NADPH by the catalytic subunit of HMGCoAR in the presence of the substrate HMGCoA, was measured spectrophotometrically. The data points represent the averages ± SEM of three independent experiments in triplicate. *, $P < 0.05$, and ***, $P < 0.0001$ vs C. C = untreated samples.

increase of the HMGCoAR protein by 170 ± 50.0 and by 177.0 ± 40.5% versus the untreated sample at 350 and 500 μM, respectively (Figure 4F).

Peptides 2 and 3 Increase HepG2 Ability to Uptake Extracellular LDL. Fluorescent LDL uptake experiments permitted us to evaluate the change of the functional capability of HepG2 cells to uptake extracellular LDL after treatment with these peptides. As shown in Figure 5, each peptide is able to
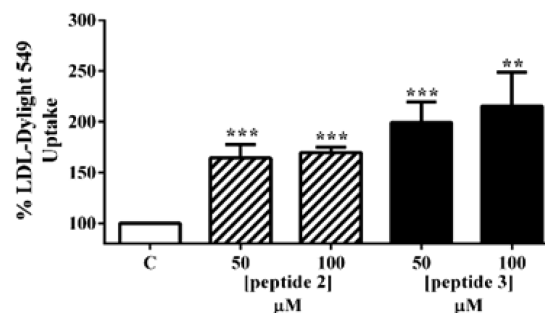

Figure 5. LDL uptake after peptide **2** and **3** treatments. HepG2 cells (3 × 10^4) were treated with 50 and 100 μM of each peptide for 24 h. LDL-Dylight 549 (10.0 μg/mL) was then incubated for additional 2 h. Excess of LDL-Dylight 549 was removed, cells washed twice with PBS, and specific fluorescent LDL-uptake analyzed by Synergy H1 (Biotek). The data points represent the averages ± SEM of three independent experiments in triplicate. **, $P < 0.001$, and ***, $P < 0.0001$, vs C. C = untreated sample.

increase the LDL uptake versus the untreated sample in a statistically significant way. In fact, the treatments with peptide **2** and **3**, at concentrations of 50 and 100 μM, led to an increase of the LDL uptake by 64 ± 29.9 and 70 ± 14.4% and 100 ± 53.1 and 215 ± 88.1%, respectively, versus the untreated sample.

■ DISCUSSION

Recently, our research group is dedicating much effort to investigate the potential bioactivity of plant food peptides[13,17,25] because this is a very promising area in functional foods.[26−28] In the framework of research aimed at investigating and characterizing the hypocholesterolemic effects of soy peptides, we have recently studied the mechanism of action through which three peptides from soy glycinin exert their hypocholesterolemic effects in HepG2 cells.[19] Unfortunately, the relevant
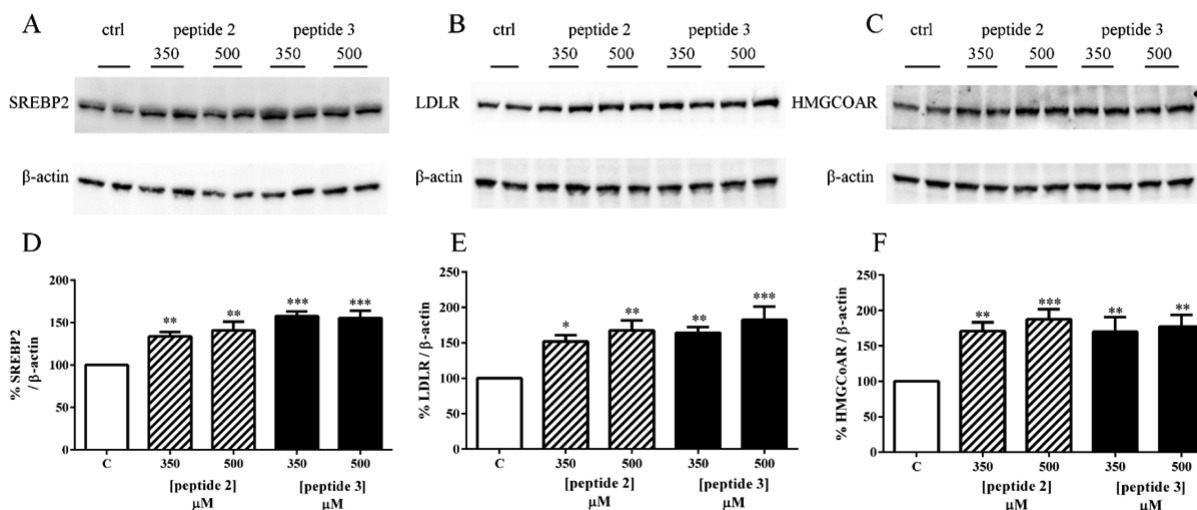
Figure 4. Effects of peptides **2** and **3** on the SREBP2, LDLR, and HMGCoAR protein levels. HepG2 cells (1.5 × 10^5) were treated with 350 and 500 μM of each peptide for 24 h, respectively. (A−C) SREBP2, LDLR, HMGCoAR, and β-actin immunoblotting signals were detected using specific anti-SREBP2, anti-LDLR, anti-HMGCoAR, and anti-β-actin primary antibodies, respectively. (D) SREBP2, (E) LDLR, and (F) HMGCoAR signals were quantified by ChemiDoc Image Lab (Biorad) and normalized with β-actin signals. Bars represent the averages of duplicate samples ± SEM of three independent experiments. *, $P < 0.05$, **, $P < 0.001$, and ***, $P < 0.0001$ vs C. C = mock treatments.

issue of the actual absorbability and bioavailability of those peptides in the gut remained unsolved.[16] The present research represents a main progress in respect to that paper because peptides **2** and **3** are very likely to be bioavailable.[22]

Another important aspect of this work is that it provides new information on peptide **1**, which has been shown to modulate LDL uptake and degradation in HepG2 cells about 15 years ago,[7] without any further verification of a direct interaction with HMGCoAR either in vitro or in silico. Our modeling study shows that the interaction of this peptide with HMGCoAR is partially impaired by its excessive length, whereas the interaction with the shorter peptide **2** encrypted in peptide **1** is much more favorable. Thus, it seems possible to hypothesize that peptide **2** may be the active part of peptide **1**.

The computational study emphasizes that a suitable HMGCoAR inhibitor should combine a negatively charged portion (residues DNDEN in peptide **2**) that mimics the HMGCoAR substrate with a more hydrophobic portion (residues YVVNP in peptide **2**). It is useful to underline that a similar situation is also observed in statins but with some differences because the statin apolar moieties mimic the pantothenic acid of coenzyme A, whereas the hydrophobic regions of these soy peptides appear to be inserted in the cofactor binding cavity.[20,21]

The in vitro experiments aimed at assessing whether peptides **2** and **3** are direct inhibitors of HMGCoAR have demonstrated for the first time that indeed these peptides, deriving either from the α or α′ subunits of β-conglycinin, are able to act as competitive inhibitors of HMGCoAR with a statin-like behavior, in agreement with the in silico investigation.

The studies carried out on human hepatic cells have shown that either peptide **2** or **3** is able to modulate cholesterol metabolism. In particular, the functional results suggest that the improved capability of HepG2 cells to uptake the LDL is strictly correlated with the molecular increase of the intra-cellular LDLR protein levels induced by these peptides upon inhibition of the HMGCoAR activity. The outcomes of these experimentations, i.e., increase of LDLR protein levels through activation of SREBP2 and enhanced cell capacity to uptake LDL cholesterol, appear to be perfectly in line with the behavior of three soy glycinin peptides, i.e., IAVPGEVA, IAVPTGVA, and LPYP, recently investigated by us.[19] In practice, we have demonstrated that the hypocholesterolemic effects can be exerted by peptides deriving from hydrolysis of either β-conglycinin and glycinin, in contrast to what has been indicated in the past.[11]

To our knowledge, this is the first work showing the molecular mechanism through which two conglycinin peptides modulate the cholesterol pathway in HepG2 cells. It may indicate how these bioavailable peptides function in cholesterol homeostasis in the liver.

■ ASSOCIATED CONTENT

ⓢ Supporting Information

The Supporting Information is available free of charge on the ACS Publications website at DOI: 10.1021/acs.jafc.5b03497.

> Overall view of the computed pose for peptides **2** (S1A) and **1** (S1B). Bidimensional scheme reporting the key interactions stabilizing the putative complex for peptide **1**. Rmsd values dissected per residue for the peptide **2** (S3A) and peptide **1** (S3B) bound to the enzyme as derived by MD runs considering all atoms. (PDF)

■ AUTHOR INFORMATION

Corresponding Author

*Tel.: +390250319372. Fax: +390250319343. E-mail anna.arnoldi@unimi.it.

Author Contributions

Experiment ideation and design: C.L. and G.V. Experiments and data analysis: experiments in HepG2 cells, C.L. and C.Z.; molecular modeling, G.V. Figure preparation: G.V. and CZ. Grant retrieval: A.A. Manuscript writing: C.L., G.V., and A.A..

Notes

The authors declare no competing financial interest.

■ ABBREVIATIONS USED

Akt, protein kinase B; 3-hydroxy-3-methylglutaryl CoA reductase; GSK3, glycogen synthase kinase 3; LDL, low-density liproteins; LDLR, low-density lipoprotein receptors; SREBP-2, sterol regulatory-element-binding protein 2

■ REFERENCES

(1) Anderson, J. W.; Johnstone, B. M.; Cook-Newell, M. E. Meta-analysis of the effects of soy protein intake on serum lipids. *N. Engl. J. Med.* **1995**, *333*, 276−82.

(2) Sirtori, C. R.; Eberini, I.; Arnoldi, A. Hypocholesterolaemic effects of soya proteins: results of recent studies are predictable from the Anderson meta-analysis data. *Br. J. Nutr.* **2007**, *97*, 816−822.

(3) Harland, J.; Haffner, T. Systematic review, meta-analysis and regression of randomised controlled trials reporting an association between an intake of circa 25 g soya protein per day and blood cholesterol. *Atherosclerosis* **2008**, *200*, 13−27.

(4) Sirtori, C. R.; Galli, G.; Lovati, M. R.; Carrara, P.; Bosisio, E.; Kienle, M. G. Effects of dietary proteins on the regulation of liver lipoprotein receptors in rats. *J. Nutr.* **1984**, *114*, 1493−1500.

(5) Lovati, M. R.; Manzoni, C.; Canavesi, A.; Sirtori, M.; Vaccarino, V.; Marchi, M.; Gaddi, G.; Sirtori, C. R. Soybean protein diet increases low density lipoprotein receptor activity in mononuclear cells from hypercholesterolemic patients. *J. Clin. Invest.* **1987**, *80*, 1498−502.

(6) Baum, J. A.; Teng, H.; Erdman, J. W. J.; Weigel, R. M.; Klein, B. P.; Persky, V. W.; Freels, S.; Surya, P.; Bakhit, R. M.; Ramos, E.; Shay, N. F.; Potter, S. M. Long-term intake of soy protein improves blood lipid profiles and increases mononuclear cell low-density-lipoprotein receptor messenger RNA in hypercholesterolemic, postmenopausal women. *Am. J. Clin. Nutr.* **1998**, *68*, 545−551.

(7) Lovati, M. R.; Manzoni, C.; Gianazza, E.; Arnoldi, A.; Kurowska, E.; Carroll, K. K.; Sirtori, C. R. Soy protein peptides regulate cholesterol homeostasis in Hep G2 cells. *J. Nutr.* **2000**, *130*, 2543−2549.

(8) Gianazza, E.; Eberini, I.; Arnoldi, A.; Wait, R.; Sirtori, C. R. A proteomic investigation of isolated soy proteins with variable effects in experimental and clinical studies. *J. Nutr.* **2003**, *133*, 9−14.

(9) Consonni, A.; Lovati, M. R.; Manzoni, C.; Pizzagalli, A.; Morazzoni, P.; Duranti, M. Cloning, yeast expression, purification and biological activity of a truncated form of the soybean 7S globulin alpha′ subunit involved in Hep G2 cell cholesterol homeostasis. *J. Nutr. Biochem.* **2010**, *21*, 887−91.

(10) Consonni, A.; Lovati, M. R.; Parolari, A.; Manzoni, C.; Morazzoni, P.; Magni, C.; Duranti, M. Heterologous expression and purification of the soybean 7S globulin α′ subunit extension region: in

vitro evidence of its involvement in cell cholesterol homeostasis. *Protein Expression Purif.* **2011**, *80*, 125−9.

(11) Duranti, M.; Lovati, M. R.; Dani, V.; Barbiroli, A.; Scarafoni, A.; Castiglioni, S.; Ponzone, C.; Morazzoni, P. The alpha' subunit from soybean 7S globulin lowers plasma lipids and upregulates liver beta-VLDL receptors in rats fed a hypercholesterolemic diet. *J. Nutr.* **2004**, *134*, 1334−1339.

(12) Aluko, R. E. Determination of nutritional and bioactive properties of peptides in enzymatic pea, chickpea, and mung bean protein hydrolysates. *J. AOAC Int.* **2008**, *91*, 947−956.

(13) Boschin, G.; Scigliuolo, G. M.; Resta, D.; Arnoldi, A. Optimization of the enzymatic hydrolysis of lupin (*Lupinus*) proteins for producing ACE-inhibitory peptides. *J. Agric. Food Chem.* **2014**, *62*, 1846−51.

(14) Martinez-Villaluenga, C.; Bringe, N.; Berhow, M.; Gonzalez de Mejia, E. Beta-conglycinin embeds active peptides that inhibit lipid accumulation in 3T3-L1 adipocytes in vitro. *J. Agric. Food Chem.* **2008**, *56*, 10533−43.

(15) Cho, S.; Juillerat, M.; Lee, C. Cholesterol lowering mechanism of soybean protein hydrolysate. *J. Agric. Food Chem.* **2007**, *55*, 10599−604.

(16) Vermeirssen, V.; Van Camp, J.; Verstraete, W. Bioavailability of angiotensin I converting enzyme inhibitory peptides. *Br. J. Nutr.* **2004**, *92*, 357−366.

(17) Lammi, C.; Zanoni, C.; Scigliuolo, G. M.; D'Amato, A.; Arnoldi, A. Lupin peptides lower low-density lipoprotein (LDL) cholesterol through an up-regulation of the LDL receptor/sterol regulatory element binding protein 2 (SREBP2) pathway at HepG2 cell line. *J. Agric. Food Chem.* **2014**, *62*, 7151−9.

(18) Mochizuki, Y.; Maebuchi, M.; Kohno, M.; Hirotsuka, M.; Wadahama, H.; Moriyama, T.; Kawada, T.; Urade, R. Changes in lipid metabolism by soy beta-conglycinin-derived peptides in HepG2 cells. *J. Agric. Food Chem.* **2009**, *57*, 1473−80.

(19) Lammi, C.; Zanoni, C.; Arnoldi, A. IAVPGEVA, IAVPTGVA, and LPYP, three peptides from soy glycinin, modulate cholesterol metabolism in HepG2 cells. *J. Funct. Foods* **2015**, *14*, 469.

(20) Istvan, E. S.; Deisenhofer, J. Structural mechanism for statin inhibition of HMG-CoA reductase. *Science* **2001**, *292*, 1160−1164.

(21) Sarver, R. W.; Bills, E.; Bolton, G.; Bratton, L. D.; Caspers, N. L.; Dunbar, J. B.; Harris, M. S.; Hutchings, R. H.; Kennedy, R. M.; Larsen, S. D.; Pavlovsky, A.; Pfefferkorn, J. A.; Bainbridge, G. Thermodynamic and structure guided design of statin based inhibitors of 3-hydroxy-3-methylglutaryl coenzyme A reductase. *J. Med. Chem.* **2008**, *51*, 3804−13.

(22) Amigo-Benavent, M.; Clemente, A.; Caira, S.; Stiuso, P.; Ferranti, P.; del Castillo, M. D. Use of phytochemomics to evaluate the bioavailability and bioactivity of antioxidant peptides of soybean *β*-conglycinin. *Electrophoresis* **2014**, *35*, 1582−9.

(23) Korb, O.; Stützle, T.; Exner, T. E. Empirical scoring functions for advanced protein-ligand docking with PLANTS. *J. Chem. Inf. Model.* **2009**, *49*, 84−96.

(24) Phillips, J. C.; Braun, R.; Wang, W.; Gumbart, J.; Tajkhorshid, E.; Villa, E.; Chipot, C.; Skeel, R. D.; Kalé, L.; Schulten, K. Scalable molecular dynamics with NAMD. *J. Comput. Chem.* **2005**, *26*, 1781−802.

(25) Boschin, G.; Scigliuolo, G. M.; Resta, D.; Arnoldi, A. ACE-inhibitory activity of enzymatic protein hydrolysates from lupin and other legumes. *Food Chem.* **2014**, *145*, 34−40.

(26) Puchalska, P.; Marina Alegre, M. L.; García López, M. C. Isolation and characterization of peptides with antihypertensive activity in foodstuffs. *Crit. Rev. Food Sci. Nutr.* **2015**, *55*, 521−51.

(27) Singh, B. P.; Vij, S.; Hati, S. Functional significance of bioactive peptides derived from soybean. *Peptides* **2014**, *54*, 171−9.

(28) Cam, A.; de Mejia, E. G. Role of dietary proteins and peptides in cardiovascular disease. *Mol. Nutr. Food Res.* **2012**, *56*, 53−66.